Stability analysis of a Light Aircraft Configuration using Computational Fluid Dynamics

Mohammed Mahdi[1, a], Yasser A. Elhassan[2,b]

[1]Sudan Master Technology, Aeronautical Research Center, Sudan

[2] Sudan Master Technology, Aeronautical Research Center, Sudan

[a]email momahdi2007@hotmail.com , [b]email yaser183@hotmail.com

Keywords: Stability Derivatives, CFD, Control, Longitudinal Stability,.Lateral Stability

Abstract.

This work aims to simulate and study the flow field around SAFAT-01 a/c using numerical solution based on solving Reynolds Averaged Navier-Stokes equations coupled with K-ω SST turbulent model.

The aerodynamics behavior of SAFAT-01 aircraft developed at SAFAT aviation complex were calculated at different angles of attack and side slip angles. The x,y and z forces and moments were calculated at flight speed 50m/s and at sea level condition. Lift and drag curves for different angles of attack were plotted. The maximum lift coefficient for SAFAT-01 was 1.67 which occurred at angle of attack 16° and Maximum lift to drag ratio (L/D) was 14 which occurred at α=3°, and the zero lift drag coefficient was 0.0342. Also the yawing moment coefficient was plotted for different side slip angles as well as rolling moment.

The longitudinal stability derivatives with respect to angle of attack, speed variation (u), rate of pitch (q) and time rate of change of angle of attack were calculated using obtained CFD results. Concerning lateral stability only side slips derivatives were calculated.

To validate this numerical simulation USAF Digital DATCOM is used to analyze this a/c; a comparison between predicted results for this aircraft and Digital DATCOM indicated that this numerical simulation has high ability for predicting the aerodynamics characteristics.

Alphabetic Symbols

A	Aspect Ratio	C_n	Yawing moment coefficient.	μ	Viscosity (kg/m/s)
C_D	Drag Coefficient	S	Wing Area (m^2)	q	Pitching rate (rad/s)
C_L	Lift Coefficient	Re	Reynolds's no.	ε	Downwash (deg)
e	Oswald Span Efficiency	x, y, z	Coordinate System	ρ	Density (Kg/m3)
u_i	Velocity	**Greek Letters**			
C_l	Rolling moment coefficient.	α	Angle of attack (deg),		
C_m	Pitching Moment coefficient.	β	Side slip angle (deg), f		
		τ	Shear Stress (Pa).		

Introduction

Over the last 30 years,industrial airplane builders developed, manufactured, sold, and supported hundreds of billions of dollars worth of commercial airplanes. During this period, it has been absolutely essential that the aerodynamicists have access to tools that accurately predict and confirm vehicle flight characteristics. Thirty years ago, these tools consisted almost entirely of analytic approximation methods, wind tunnel tests, and flight tests[1]. With the development of increasingly powerful computers, numerical simulations and various approximations of the Navier-

Stokes equations began supplementing these tools. Petra Aumann et.al [2] said that by the end of the 1980's, AIRBUS-D had put much validation effort into high level CFD technology. By the end of the 1990's, CFD itself was fully accepted and used within the aerodynamic design and data processes.

O.Brodersen and A.Sturmer[3]from DLR Institute of design aerodynamics, Germany in the conference of AIAA Drag Prediction Workshop uses Navier Stokes solver to predict the drag of a wing body combination they compare their CFD results with other previous work in other commercial codes and they validate their work by wind tunnel testing of the wing-model model.

In this paper so, a general aviation aircraft namely SAFAT 01 is to be analyzed from an aerodynamics approach to find the forces and moments coefficients which are to be used to conduct open and closed loop control of the aircraft.

Mathematical Model

For analyzing the studied wing of SAFAT-01, the flow is assumed to be incompressible due to the maximum speed is 50(m/s). so only Navier stokes equations with the K-Omega SST and continuity equation are solved simulatinousely.

Mass conservation law:

$$\frac{\partial(u_i)}{\partial x_j} = 0 \tag{1}$$

Navier-Stokes Equations: These equations were employed in the following form:

$$\frac{\partial \vec{q}}{\partial t} + \frac{\partial \vec{E}}{\partial x} + \frac{\partial \vec{F}}{\partial y} + \frac{\partial \vec{G}}{\partial z} = \frac{\partial \vec{R}}{\partial x} + \frac{\partial \vec{S}}{\partial y} + \frac{\partial \vec{T}}{\partial z} \tag{2}$$

Where

$$\vec{q} = \begin{bmatrix} \rho \\ \rho u \\ \rho v \\ \rho w \end{bmatrix} \quad \vec{E} = \begin{bmatrix} \rho u \\ \rho u^2 + p \\ \rho uv \\ \rho uw \end{bmatrix} \quad \vec{F} = \begin{bmatrix} \rho v \\ \rho uv \\ \rho v^2 + p \\ \rho vw \end{bmatrix} \quad \vec{G} = \begin{bmatrix} \rho w \\ \rho uw \\ \rho vw \\ \rho w^2 + p \end{bmatrix} \quad \vec{R} = \begin{bmatrix} 0 \\ \tau_{xx} \\ \tau_{xz} \\ \tau_{xz} \end{bmatrix} \quad \vec{S} = \begin{bmatrix} 0 \\ \tau_{yx} \\ \tau_{yy} \\ \tau_{yz} \end{bmatrix} \quad \vec{T} = \begin{bmatrix} 0 \\ \tau_{zx} \\ \tau_{zy} \\ \tau_{zz} \end{bmatrix}$$

*Turbulence model equation***.** Selection of turbulence model depends on type of grid i.e., structure or unstructured grid. Accordingly for the present simulation K-omega SST turbulent model was used for the purpose of turbulence closure. This model has wide spread popularity among CFD researchers. For more information about this model see F. R. Menter et.al [4]. He state that this model is more accurate than k-epsilon specially near wall layers, and for flows with moderate adverse pressure gradients

Geometry and meshing:

In this section the CFD analysis scheme of SAFAT-01 will be demonstrated, first the CATIA solid model is created to be suitable for CFD analysis, this required additional attention in creating the model by minimum faces and volumes, to prevent bad quality elements. The model is shown in fig.1 below

Fig.1 SAFAT-01 3-Views

Grid Generation. Computational domain is shown in fig 3.7 with specified boundaries, the domain is created big enough to set farfield values of velocity and pressure, farfield require the lower effect of wing downwash and wake behind wing and a/c, the domain dimension is 6* span radius of the sphere and cylinder, 11*span behind a/c .

Fig. 2-a shows the mesh elements of SAFAT-01 components, a fine mesh is focused near a/c surface to smooth surfaces as well as considering the boundary layer effect, the interval size of the element is almost 2.5 (mm), which is created inside GAMBIT , grid is unstructured type with triangles and tetrahedral in the surface and volume meshes, approximately 4 million cells is created in the computational domain of SAFAT-01.

The computational domain and boundary conditions definitions is shown in fig. 2-b , the free stream velocity and angles of attack or side slip is entered by defining velocity inlet conditions.

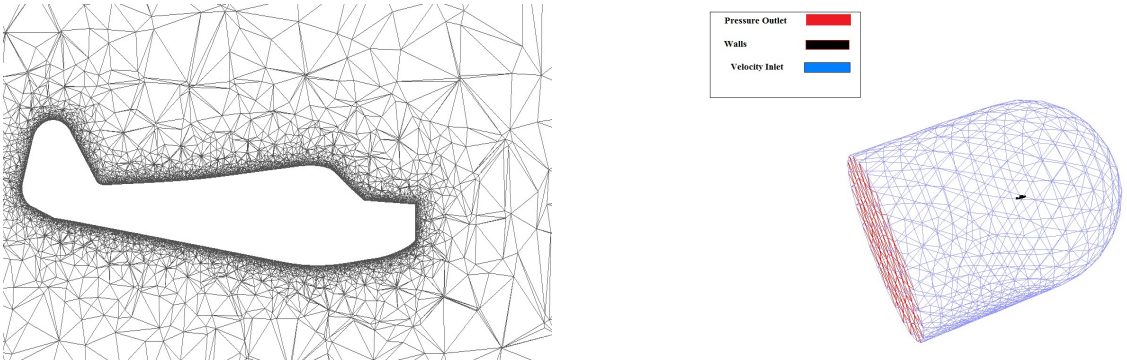

Fig. 2 a) grid elements for SAFAT-01 *b) Computational domain and boundary conditions*

Results and Discussions

Fig. 3 a illustrates the relation between lift coefficient and angle of attack, the relation is calculated using CFD code and USAF digital DATCOM at Re=5.4×10^6 and free stream velocity equal to maximum level speed 180km/hr. This figure shows that both CFD and digital DATCOM results are very close to each other but digital DATCOM lift curve slope is greater than CFD lift curve slope (table 1) in linear zone. Both CFD and USAF digital DATCOM predict stall occurs at α=16(deg), but CFD shows that post-stall region (α>16 deg) has greater lift with comparison of digital DATCOM results; which shows instantinous decrement in lift forc at α>16(deg).

Fig. 3.b shows the relation between pithcing moment coeffient and the angle of attack, which calculated using CFD code and USAF Digital DATCOM. The moment center is assumed to be at wing mean aerodynamics quarter chord. CFD and digital DATCOM results shows a linear relation,

There are differences in pitching moment curves between CFD simulation and DATCOM data which the CFD data shows a steep curve than DATCOM at Fig.3.b.

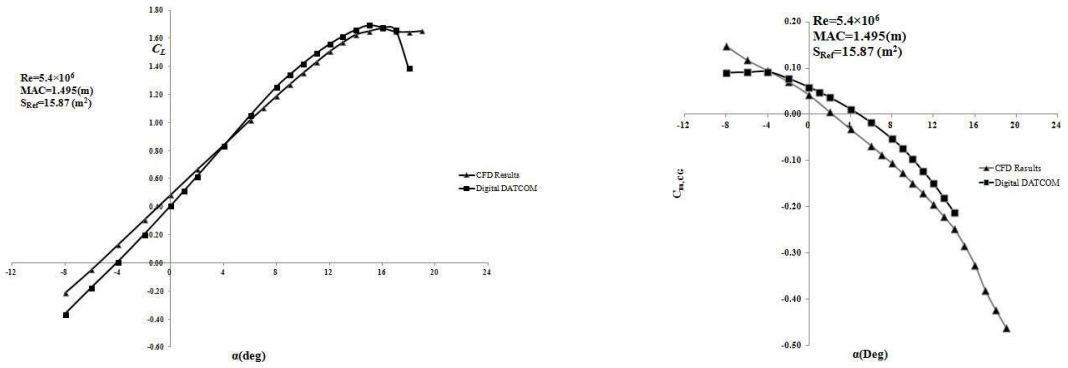

(a (b

Fig. 3 a) Lift Coefficient Vs AOA b) pitching moment Vs AOA

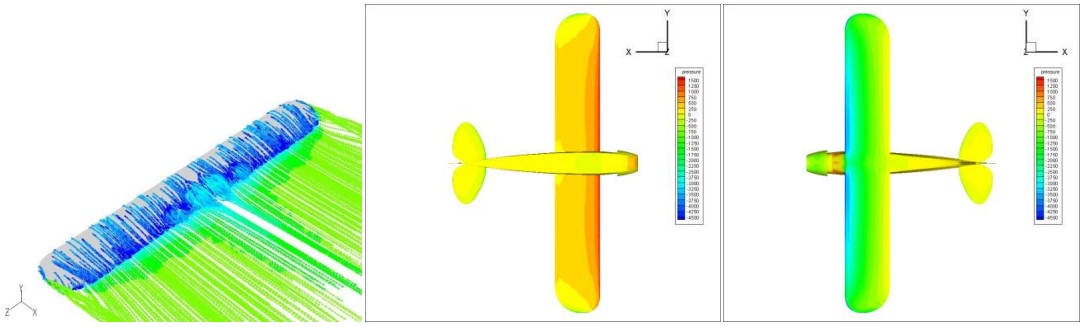

(a) (b) (c)

Fig.4 flow field at α=12(deg) (a) flow pathlines (b) Pressure contours lower surfaces (c) Pressure contours upper surfaces

Fig. 4-a shows the flow pathlines over the upper surface of wing at *α=16.* This figure indicates an existence of vortex on upper surface and tip vortices. The vortices zones are captured by the pencil and zoomed as shown in Fig. (4.16). This figure reveals that, the separation occurs near wing root first and starts to extend spanwisely by increasing angle of attack. Due to vortices near the wing root trailing edge it is predicted that wing flap may not be effective at *α>16.*

Fig 4.b,c illustrates the pressure contours in upper and lower surfaces captured at α=16º of SAFAT-01. We observe that the pressure on upper surface (a) is lower than the pressure on lower surfaces (c) due to the positive wing camber and the presence of wing incidence angle.

The downwash is estimated from CFD, that rake line is constructed along the aerodynamics axis of the HT, and then the downwash effect on the tail is plotted vs HT semi span.

According to Biot-Savart law the vortex will induce downwash due to induced velocity and given by

$$\varepsilon = -\tan^{-1}\left[\frac{V_Z \cos\alpha - V_x \sin\alpha}{|V|}\right] \qquad 4$$

Stability Derivatives Results:

The methods described in [5] is used to find the stability derivatives coefficientsusing steady state results of CFD, and then compared with results obtained from USAF digital DATCOM.

Table 1 Longitudinal and lateral steady state derivatives.

Longitudinal Stability Derivatives-Steady State								
	$C_{D\alpha}$ ***(1/rad)***	$C_{L\alpha}$ ***(1/deg)***	$C_{m\alpha}$ ***(1/deg)***	C_{Lq} ***(1/rad)***	C_{mq} ***(1/rad)***	C_{Du} *	C_{Lu}	C_{mu} **
CFD	0.25	0.0900	-0.0185	0.0281	-0.0740	0.0000	-1.3199	-0.0026
Digital DATCOM	0.2218	0.1044	-0.0106	0.0677	-0.0768	0	-1.1	-0.005
Lateral Stability Derivatives								
	$C_{n\beta}$ ***(1/deg)***		$C_{y\beta}$ ***(1/deg)***			$C_{l\beta}$ ***(1/deg)***		
CFD	0.00072		0.0077			-0.005		
Digital DATCOM	0.0003		-0.0073			-0.0014		
Longitudinal Stability Derivatives-derivatives related to time rate of change of the angle of attack								
	$C_{L\dot{\alpha}}$ **(1/deg)**				$C_{m\dot{\alpha}}$ **(1/deg)**			
CFD	-0.0158				-0.02			
Digital DATCOM	-0.0154				-0.0405			

Table 1 show the estimation of stability derivatives using CFD results and digital DATCOM, only the longitudinal stability coefficients are derived, because the longitudinal stability is the most series and important than lateral stability. Then it is easily to find longitudinal dynamic stability using the equation of motion in longitudinal axis. Due to incompressibility effect the terms C_{Du} is zero as well as C_{mu}.

The values of non-dimensional coefficient obtained by assuming the body is rigid, and the coordinate system x,z lies on the axis of symmetry, so y is spanwise and z vertical where x is longitudinal. This explained when deriving the forces from FLUENT.

The derivatives related to time rate of change of the angle of attack is founded using Steady state CFD results with the formulae defined in [3] and using the downwash predicted using CFD to estimate the values of $C_{L\dot{\alpha}}$ and $C_{m\dot{\alpha}}$.

Conclusion:

In this paper the stability derivatives is calculated using Reynolds Averaged Navier Stokes Equations (RANS) and USAF digital DATCOM, The analysis work was done to report the aerodynamic performance of SAFAT-01 intended to be capable for low subsonic operation. The 3-D model generated by CATIA became the basis of the CFD model for predicting the pressure and flow field around the a/c, concerning CFD analysis the incompressible solution of RANS coupled with SST turbulent model is applied to SAFAT-01, the a/c is analyzed in a wide range of angles of attack and side slip angles in both CFD and DATCOM, wing downwash effect on the tail is calculated for preliminary calculations of SAFAT-01., which subsequently develops to be the

aerodynamic load. This analysis carried at V=50m/s (180 km/hr) which represents the loitering and the cruising phase of the mission profile. From the C_L curves obtained from CFD coupled with visualization Flow Pathlines figures, it can be concluded that the maximum lift is occurred at α around 16º.

References

[1] Edward N. Tinoco, "Thirty Years Of Development And Application Of CFD At Boeing Commercial Airplanes, Seattle", 16th AIAA Computational Fluid Dynamics Conference, 2003.

[2] Petra Aumann and Klaus Becker," MEGAFLOW for AIRBUS-D Applications and Requirements", AIAA, DLR, (2009),.

[3] O. Brodersen, A. Sturmer, "Drag Prediction Of Engine–Airframe Interference Effects Using Unstructured Navier–Stokes Calculations", 19th AIAA Applied Aerodynamics Conference, 2001.

[4] Florian R. Menter, "Improved Two-Equation *k-ω* Turbulence Models for Aerodynamic Flows", NASA Technical Memorandum 103975.

[5] Bernard Etkin, " Dynamics of Flight Stability and Control", 3rd Ed, 1996, John Willey & Sons, pp 129-156

[6] H.K.Versteeg ,W.Malalasekera, "An Introduction to Computational Fluid Dynamics The Finite Volume Method", Pearson Education Limited, 2007, Harlow, England.

[7] Robert P. Little, "Flight Simulator Database Population from Wind-Tunnel and CFD Analysis of a Homebuilt Aircraft", MSc These, California Polytechnic State University, San Luis Obispo.

[8] H.Schlichting, K.Gersten, "Boundary Layer Theory", McGraw Hill, 2000, N.Y.

[9] Courant, R., Isaacson, E., and Rees, M. (1952). "On the Solution of Nonlinear Hyperbolic Differential Equations by Finite Differences", Comm. Pure Appl. Math., 5, 243-255.

[10] John Anderson, Jr. "Fundamentals of Aerodynamics", 5th edition, McGraw Hill, (2010), 981-1040.

[11] Patankar, S. V."Numerical Heat Transfer and Fluid Flow.:Taylor & Francis.

[12] AIAA 3rd Drag Prediction Work Shop Presentations by Marviplis and Tahran, http://aaac.larc.nasa.gov/tsab/cfdlarc/aiaa-dpw/Workshop3/workshop3.html, Retrived at 1st March 2011.